Impact of Watershed Geomorphic Characteristics on the Energy and Water Budgets

GIACOMO BERTOLDI AND RICCARDO RIGON

Department of Civil and Environmental Engineering, CUDAM, University of Trento, Trento, Italy

THOMAS M. OVER

Department of Geology/Geography, Eastern Illinois University, Charleston, Illinois

(Manuscript received 2 March 2005, in final form 4 October 2005)

ABSTRACT

The GEOtop model makes it possible to analyze the short- and long-term effects of geomorphic variation on the partitioning of the lateral surface and subsurface water and surface energy fluxes. The topography of the Little Washita basin (Oklahoma) and of the Serraia basin (Trentino, Italy) have been used as base topographies from which virtual topographies with altered slopes and elevations have been created with corresponding modifications of the soil thickness and the extension of the channel network, according to applicable geomorphological theories, in order to quantify the contribution of these topographic features to the spatial and temporal variability of energy and water fluxes. Simulation results show that both a more extended channel network and more accentuated slopes cause an increase in the discharge balanced by a diminution of the evapotranspiration. The diminution of the latent heat flux is balanced by the increase in the sensible heat flux. Net radiation shows a minor sensitivity to topography. Evaporative fraction, on the contrary, is shown to be strongly dependent on geomorphic characteristics. The results confirm the importance of including an adequate treatment of topography in large-scale land surface models.

1. Introduction

Variability in land surface properties due to topography, soil characteristics, and the distribution of vegetation can create significant heterogeneities that affect large-scale soil moisture dynamics, runoff production, and surface energy fluxes (Liang et al. 1994). In turn, many studies (e.g., Avissar and Pielke 1989; Entekhabi et al. 1992; Rodriguez-Iturbe et al. 1999; Warrach et al. 2002) have shown that the heterogeneity of soil moisture can have significant feedbacks on atmospheric fluxes, temperature, and precipitation at the mesoscale. Therefore, understanding the interplay of these effects is of great interest in climatology, weather forecasting, and hydrology.

Topography directly controls the celerity of the surface flow (which is proportional to the square root of the local slope) and of the subsurface flow (which is proportional to the local slope and water content). Moreover, topography affects the surface radiation balance: slope, aspect, and surrounding mountains control the amount of incident direct solar radiation, and lower-elevation regions in mountainous basins have a smaller portion of visible sky and therefore less incoming shortwave radiation from the sky but more incoming longwave radiation from the surrounding mountains. Higher elevation regions have a lower air temperature due to the decrease of air temperature with elevation, which also affects the partitioning of fluxes. Figures 1 and 2 visualize these and other effects in the small mountain catchment of Serraia, Italy: the highest evapotranspiration (E_T) values are in the bottom of the main valley (where indeed there are a lake and a wetland), and the lowest values are in north-facing, high-elevation areas. Finally, topography affects soil thickness, which determines water storage capacity.

Despite significant efforts that have been made in order to incorporate hydrologically based lateral water redistribution processes in large-scale land surface models (LSMs) (Lakshmi et al. 2001) [to cite a few: Entekhabi and Eagleson (1989); the Variable Infiltration Capacity (VIC) model (Liang et al. 1994); Famiglietti and Wood (1994); and Wigmosta et al. (1994)], the

Corresponding author address: Giacomo Bertoldi, Dept. of Civil and Environmental Engineering, CUDAM, University of Trento, Via Mesiano 77, Trento, TN 38050, Italy.
E-mail: giacomo.bertoldi@ing.unitn.it

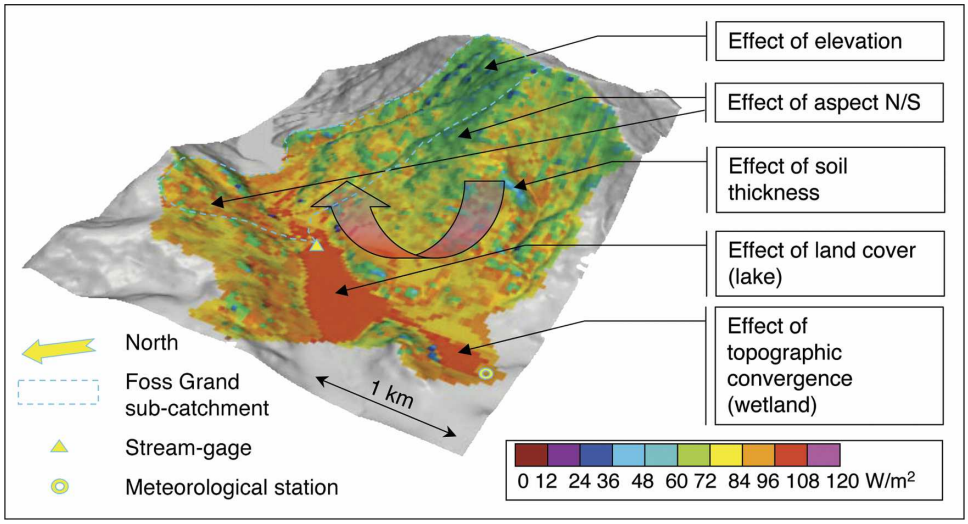

FIG. 1. Simulated daily evapotranspiration for the Serraia basin, Italy, for 20 May 2000. The simulation was performed using the GEOtop model at 40-m grid resolution. Notice the elevation effect (areas more elevated have less evaporation), the aspect effect (more evaporation from southern slopes, left part of the image), and the topographic convergence effect on water availability (at the bottom of the valley). The spatial variability of surface energy fluxes can induce atmospheric local circulation effects (indicated with an arrow), with feedbacks on the surface fluxes themselves.

advantage of a topographically controlled runoff simulation in LSMs has been overlooked except in a few works (e.g., Warrach et al. 2002), and explicit assessment of the role of topographically controlled variability on surface fluxes has, to our knowledge, never been carried out.

As a contribution to the understanding of the effect of topographic changes on the surface fluxes, this paper examines the role of topography and geomorphology (in particular the extension of the channel network and the soil depth) in controlling the water storage in the hillsides, on the rate of production of surface and subsurface runoff, and consequently on the evapotranspiration. For explicitly representing these phenomena, the distributed model GEOtop (Rigon et al. 2006; Zanotti et al. 2004) is used. Even though a fully explicit approach, such as GEOtop uses, would seem infeasible for global-scale application, this approach can give a quantitative estimate of the errors involved in neglecting topographic heterogeneity and can give some ideas

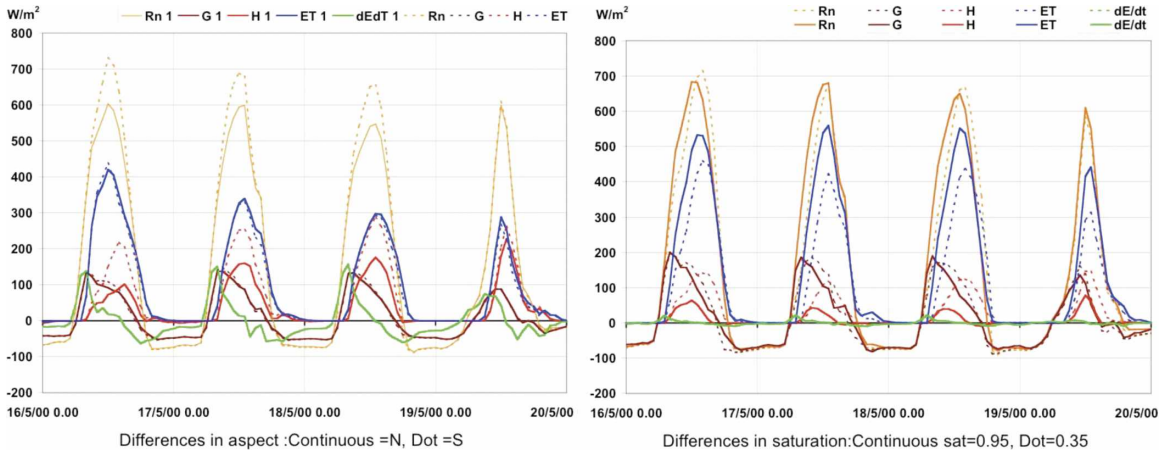

FIG. 2. Simulated surface energy balance components for two locations in the Serraia basin with the same soil properties and elevation but differing in other parameters: R_n, net radiation, G, ground heat flux, H, sensible heat flux, and dE/dt, energy storage variation in the surface layer. (left) Same land use (forest) and soil saturation but different aspect; (right) same land use (grass) and aspect but different soil saturation.

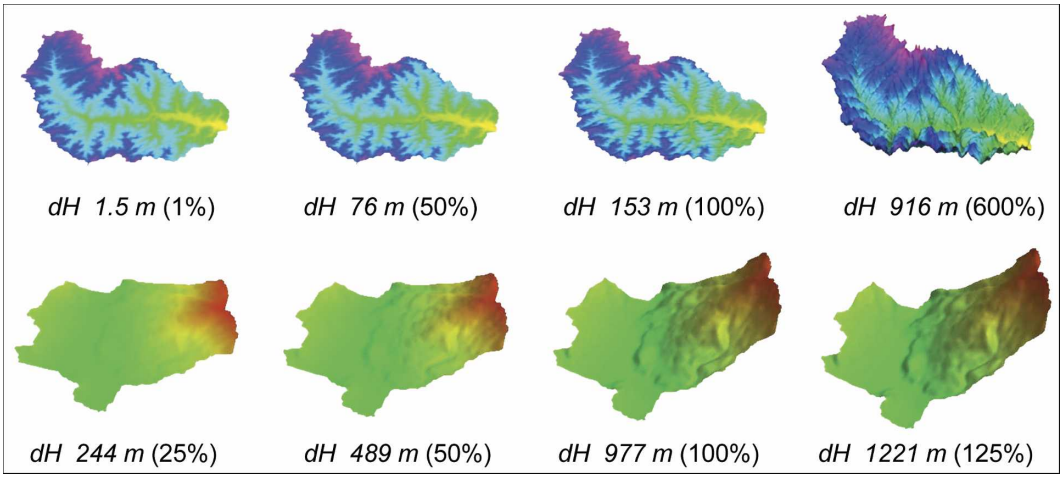

FIG. 3. Variation of topography in the (top row) Little Washita watershed (603 km^2) and (bottom row) Serraia catchment (9 km^2). Virtual topographies with altered slopes and elevation differences (basin relief) *dH* have been created to determine how changes in topography affect flux partition at catchment scale. Percentages refer to the fraction of the actual basin relief.

regarding how to parameterize its effects at large scale. Figure 1 also suggests that spatial heterogeneity of surface fluxes can induce local wind circulations with possible feedback effects on the atmospheric boundary layer. To treat this problem, a possible approach is to use large eddy simulation (LES) to simulate turbulent processes, as for example in Albertson et al. (2001); however, this aspect of the dynamics is beyond the scope of this paper.

This paper describes the results of numerical experiments consisting of high-resolution spatial simulations using GEOtop with real and modified topography. These experiments were conceived in order to highlight the effect of topography on the dynamic elements that are relevant to the partition of hydrologic fluxes, with special regard to the quantification of the role of lateral distribution on the total large-scale balance. Water and energy budgets of annual and monthly durations are analyzed. The annual duration experiments are analyzed at a monthly scale; the monthly experiments are analyzed at event time scales. In the attempt to minimize the influence of local factors in the interpretation of the results, two basins in different climatic and geomorphic areas were chosen. In the first part of this article, data and simulations from the Little Washita watershed (Oklahoma), where the GEOtop model has been tested against discharge (see Rigon et al. 2006) and surface flux measurements, are used to analyze the individual and combined effects of soil thickness, river network extension, and slope on the water and surface energy balance surrounding a summertime rainfall event (with a total simulation duration of about one month) and for the entire year of 1997. In the second part, analysis of an annual simulation of a small mountain catchment in the Italian Alps (the Serraia watershed in Trentino, Italy), very different from the Little Washita in geomorphological and climatic conditions, is presented.

2. Methods

To determine how changes in topography affect the partitioning of water and energy fluxes at the catchment scale, it is necessary to vary the topography. Since this cannot be easily performed in nature, virtual topographies with altered slopes and elevations have been created as shown in Fig. 3. These modifications, besides altering the primary geometrical aspects of the terrain, have strong geomorphological feedbacks, causing modifications of the soil thickness and the channel network extension (Rodriguez-Iturbe and Rinaldo 1997; Dietrich et al. 1993) that must be considered in order to obtain a realistic, even if conceptual, model. In fact, the hydrologically active soil thickness and the channel network extension can also be, in a conceptual experiment, treated separately.

The change in thickness of the hydrologically active soil layer is here modeled according to Stocker (1998), who further developed the model of Heimsath et al. (1997). This model assumes that in the condition of a stationary balance between soil production and erosion, the soil thickness h in the convex zones ($\nabla^2 z < 0$) is obtained through the following expression:

$$h = -\frac{1}{m}\ln\left(-\frac{k\nabla^2 z}{P_0 \cdot \rho_r/\rho_s}\right) = \frac{1}{m}\ln\left(\frac{\nabla^2 z_{\text{crit}}}{\nabla^2 z}\right), \quad (1)$$

where z is the surface elevation, ∇^2 is the Laplacian operator (L^{-2}), $\nabla^2 z_{crit} = -P_0\, \rho_r/(\rho_s\, k)$ (L^{-1}) is the critical curvature that corresponds to bare bedrock, P_0 ($L\ T^{-1}$) is the soil production for null soil depth, m the decay rate with soil depth of soil production (L^{-1}), ρ_r ($M\ L^{-3}$) and ρ_s ($M\ L^{-3}$) are the rock and soil bulk densities, respectively, and k ($L^2\ T^{-1}$) is the soil diffusivity (M, L, and T are MKS units). Equation (1)—derived in the appendix under the assumption of no subgrid topographic variability, resulting in no loss of generality for the present simulations—refers to a soil-mantled landscape, and the linear diffusion law is used as the effect of many diverse geomorphologic processes that cumulate according to the central limit theorem. For areas with slopes steeper than a critical angle (depending on lithology), soil can form only temporarily. In these areas there is usually exposed rock, and debris flows and landslides dominate the landscape evolution. In the concave zones, the soil thickness depends on the basin's geologic history, and therefore this relationship cannot be applied. In the present paper a fixed soil thickness is assumed for these areas.

The extent of the channel network is modeled here according to Dietrich et al. (1993), who assume, like many authors, that the incision of channels takes place only if the stress tangent to the bottom exceeds a critical threshold value (τ_{crit}), which can be expressed according to

$$\tau = \alpha S(\mathbf{x})^q \cdot |\nabla z|^n > \tau_{crit}, \tag{2}$$

in which $\mathbf{x}$ is the position of the point considered, S is the contributing area to $\mathbf{x}$ (S is a proxy for the discharge in channel-forming events), ∇z (dimensionless) is the modulus of the gradient (i.e., the local slope), and α, q, and n are coefficients that depend on soil characteristics and on the concentration of runoff in unresolved rills (Carson and Kirkby 1972; Willgoose et al. 1991; Prosser and Abernethy 1996). Together, the soil depth and channel network extension relations indicate that the steeper the slope of a basin, the less soil is available on the hillslopes and the greater the drainage density, if the lithology is the same.

Quantification of further geomorphic alterations caused by changing elevations, such as modification of fining in the streambed and of the rate of pedogenesis (which is, in the present theory, embedded in P_0) and their interplay, are far beyond our current knowledge and in the present paper are neglected. In fact, the simulations performed represent a first exploration of the possibilities of investigation of hydrologic processes permitted by a distributed model like GEOtop. Strictly speaking, the results presented are exactly valid only with reference to the hypotheses that form the basis of the model and to the conditions of simulations specified; nevertheless the authors believe that the results obtained can be considered of general value.

The procedure used to modify elevations is based on changing slopes by a multiplicative factor as presented in the next pages. This procedure maintains unaltered existing slope-area scaling properties of the basin since the aggregation structure of the drainage directions and consequently the contributing area remains unchanged. It also leaves unchanged the sign of curvatures (i.e., of the Laplacian of the topography); thus the locations and the extents of hillslopes and valleys remain the same.

To analyze the effects of the variation of the topography on the energy and water balance, series of simulations have been performed on three sets of modified topographies: (i) varying the soil depth alone (S1), (ii) varying the channel network extension alone (S2), and (iii) varying the elevations (and slopes) with effects on the soil depth and channel network extension (S3). Simulations of all three types, S1, S2, and S3, were performed for the Little Washita basin, but only type S3 for the Serraia basin. Each set of simulations was forced with the same periodic meteorological conditions repeatedly until a dynamic equilibrium condition was reached. This allows each terrain, soil depth, and channel network combination to dynamically adapt to the forcing and minimizes initialization errors.

a. S1 "soil" simulations: Variation of soil thickness

In this series of simulations, soil thickness has been varied by changing the critical curvature $\nabla^2 z_{crit}$ according to

$$\nabla^2 z'_{crit} = \frac{\nabla^2 z_{crit}}{c}, \tag{3}$$

where $\nabla^2 z_{crit}$ is the observed critical curvature value, $\nabla^2 z'_{crit}$ is the modified critical curvature value, and c is a multiplicative factor. Substituting z'_{crit} into (1) results in a decreased soil depth by an amount equal to $(\ln c)/m$ [i.e., $h' = h - (\ln c)/m$] (see Table 1).

b. S2 "network" simulations: Variation of the river network extension

In this series of simulations, the critical shear stress τ_{crit} value is decreased again by dividing by a factor c; that is,

$$\tau'_{crit} = \frac{\tau_{crit}}{c}. \tag{4}$$

TABLE 1. Summary of the geomorphic parameters of the S1 ("soil": soil thickness variation) series of GEOtop simulations in the Little Washita basin.

Simulation name	Multiplicative factor C	Basin relief dH (m)	$\nabla^2 z_{crit}$ (m^{-1})	Average soil thickness (m)	τ_{crit}/α (m)	River network length (km)
S1-0.01	0.01	153	6.46	2.00	0.15	271
S1-0.05	0.05	153	1.29	1.85	0.15	271
S1-0.25	0.25	153	0.26	1.74	0.15	271
S1-0.50	0.5	153	0.13	1.68	0.15	271
S1-1	1	153	0.064	1.61	0.15	271
S1-2	2	153	0.032	1.55	0.15	271
S1-4	4	153	0.016	1.50	0.15	271
S1-5	5	153	0.013	1.48	0.15	271
S1-6	6	153	0.011	1.46	0.15	271

A decrease in the value of τ_{crit} causes a larger channel network to be identified (see Table 2). Because the channel network cannot extend outside the concave areas, a limit to c increase can be determined, being c_{max}, the value in which channels would start in convex areas.

c. *S3 "slope" simulations: Variations in slope and corresponding changes in river network extension and soil thickness*

In this series of simulations, the slope has been modified according to a multiplicative factor c so that $\nabla z' = c\nabla z$. The height varies accordingly, since it can be seen as the summation of height jumps along the drainage paths; that is,

$$H_i' = \sum_j c\nabla z_j \, dr_j, \tag{5}$$

where dr_j is the jth pixel side and the summation is over all the points downhill of the pixel i. However, the mean basin elevation, H_m, is maintained constant so that climatic effects, due to the temperature decrease with the elevation, are minimized. Consequently, the elevation H varies locally according to the affine transformation

$$H' = cH + H_m(1 - c). \tag{6}$$

Power-law slope-area relationship scaling is preserved by construction if it exists. In fact, if $\nabla z \propto A^{\gamma}$, where A is, as usual in geomorphometric analysis, the planar projection of the contributing area, then, for the modified topography, is $\nabla z = c\nabla z \propto A^{\gamma}$.

Because the slope varies, the extension of the channel network varies according to Eq. (2), and so does the soil thickness in the convex zones as well, according to (1) (see Tables 3 and 4). Using the set of c values reported in Tables 1–4, for the three series of simulations, the simulations of the S3 series have the same storage capacities as those of the S1 series (having the same critical curvature at the same point), but with different slopes, and the same channel network extension as the S2 simulations (having the same τ_{crit} values). Note that one member of each series, the simulation where $c = 1.0$, is the base simulation, as it uses the real topography of the basin.

3. Water and energy budgets in the Little Washita watershed

The GEOtop model was applied, using a grid resolution of 200 m, to the 603-km^2 portion of the Little

TABLE 2. Summary of the geomorphic parameters of the S2 ("net": river network variation) series of GEOtop simulations in the Little Washita basin.

Simulation name	Multiplicative factor C	Basin relief dH (m)	$\nabla^2 z_{crit}$ (m^{-1})	Average soil thickness (m)	τ_{crit}/α (m)	River network length (km)
S2-0.01	0.01	153	0.064	1.61	15	0.24
S2-0.05	0.05	153	0.064	1.61	3	0.48
S2-0.25	0.25	153	0.064	1.61	0.6	40.6
S2-0.50	0.5	153	0.064	1.61	0.3	115
S2-1	1	153	0.064	1.61	0.15	271
S2-2	2	153	0.064	1.61	0.075	623
S2-4	4	153	0.064	1.61	0.0375	1214
S2-5	5	153	0.064	1.61	0.03	1342
S2-6	6	153	0.064	1.61	0.025	1410

TABLE 3. Summary of the geomorphic parameters of the S3 ("slope": slope, river network, and soil thickness variation) series of GEOtop simulations in the Little Washita basin.

Simulation name	Multiplicative factor C	Basin relief dH (m)	$\nabla^2 z_{crit}$ (m^{-1})	Average soil thickness (m)	τ_{crit}/α (m)	River network length (km)
S3-0.01	0.01	1.5	0.064	2.00	0.15	0.24
S3-0.05	0.05	7.6	0.064	1.85	0.15	0.48
S3-0.25	0.25	38	0.064	1.74	0.15	40.6
S3-0.50	0.5	76	0.064	1.68	0.15	115
S3-1	1	153	0.064	1.61	0.15	271
S3-2	2	305	0.064	1.55	0.15	623
S3-4	4	611	0.064	1.50	0.15	1214
S3-5	5	763	0.064	1.48	0.15	1342
S3-6	6	916	0.064	1.46	0.15	1410

Washita watershed upstream of U.S. Geological Survey (USGS) stream gauge 07327550, located east of Ninnekah, Oklahoma. The simulations made use of data from the Southern Great Plains 1997 Hydrology Experiment (SGP97; Jackson et al. 1999), which took place during the summer of 1997 in central Oklahoma.

The GEOtop model of the Little Washita watershed was calibrated against the SGP97 discharge and surface flux measurements, and the simulated soil moisture patterns were validated against the Electronically Scanned Thinned Array Radiometer (ESTAR) soil moisture maps obtained during SGP97 (Jackson et al. 1999). The entire year of 1997 was simulated, but to allow for better comparison with SGP97 measurements, the model was calibrated to the streamflow from 27 June to 22 July 1997, and this period is analyzed in greater detail. This calibrated simulation has been assumed to be the reference state of the basin for the purposes of the comparisons discussed here. The results of this "base" simulation are given in detail in Rigon et al. (2006). For the base simulation, the soil thickness in the concave areas was fixed at 2.0 m, while it varies according to Eq. (1) in the convex zones, with a basin-averaged value of 1.61 m. In the other simulations, the soil thickness in the concave areas remains fixed at 2.0 m, but in the convex zones the soil thickness varies depending on slope. The parameters q and n in Eq. (2), used for channel network definition, have been set to 0.5 and 1, respectively, and the parameter α has been calibrated to match the extracted river network with the real one. The soil parameters, such as density, porosity, and hydraulic conductivity, were assumed to vary across the basin according to previous studies of the area (Mohanty et al. 2000; Mohr et al. 2000). Vegetation cover was defined according to the map of Doraiswamy (2001). More details on the specification of soil and vegetation parameters are given in Rigon et al. (2006).

The simulation period used for the calibration is a dry summer period during which, however, a rainfall event brought considerable moisture to the basin, which subsequently dried out again. A comparison of the measured and simulated discharge hydrographs and associated rainfall is given in Fig. 4 of Rigon et al. (2006). The water balance for this simulation period is reported in Fig. 5 of Rigon et al. (2006). It shows that during the period considered the basin loses water more by evaporation than by stream discharge and, as that implies, water from the major rain event is mostly stored in the basin soils and removed by evaporation rather than running off shortly after the rain event. Total estimated precipitation over the period was 84 mm, while total measured discharge was 12 mm, and total simulated evapotranspiration (ET) was 96 mm,

TABLE 4. Summary of the S3 ("slope": slope, river network, and soil thickness variation) series of GEOtop simulations in the Serraia catchment.

Simulation name	Multiplicative factor C	Basin relief dH (m)	$\nabla^2 z_{crit}$ (m^{-1})	Average soil thickness (m)	τ_{crit}/α (m)	River network length (km)
S3-0.25	0.25	244	0.064	0.79	5	0.05
S3-0.40	0.4	391	0.064	0.77	5	3.04
S3-0.50	0.5	489	0.064	0.76	5	6.71
S3-0.65	0.65	635	0.064	0.73	5	8.55
S3-0.75	0.75	733	0.064	0.73	5	10.1
S3-1	1	977	0.064	0.71	5	14.8
S3-1.25	1.25	1221	0.064	0.70	5	21.3

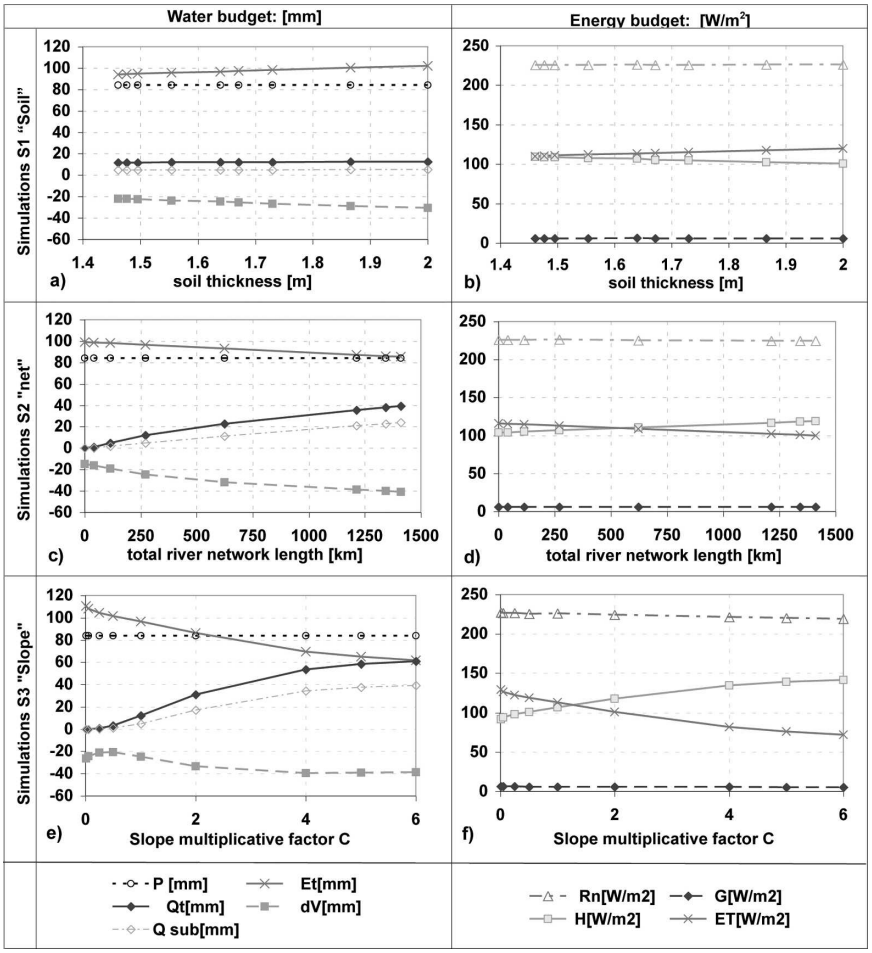

FIG. 4. Simulated (first column) total water budget and (second column) energy budget of the Little Washita watershed during the period 27 June–22 July 1997. (first row) Results of S1 simulations having soil thickness variation. (second row) Results of S2 simulations having river network variation. (third row) Results of S3 simulations having slopes modified by the factor c and consequent river network extension and soil thickness variation. Water budget components are precipitation P, evaporation E_T, change in soil water content dV [i.e., $V(t_{\text{final}}) - V(t_{\text{initial}})$, where t_{final} and t_{initial} are last and first time steps of the simulation], total discharge Q_t, and subsurface flow Q_{sub}, where $P = Q_t + E_T + dV$. Energy budget components are net radiation R_n, ground heat flux G, and sensible and latent heat fluxes, H and E_T, respectively, where $R_n = G + H + E_T$.

implying a decrease in basin soil moisture storage of 24 mm. Total estimated precipitation over the entire year was 943 mm, while total measured discharge was 139 mm, and total simulated ET was 808 mm, implying a decrease in basin soil moisture storage of 12 mm.

a. Results of simulations S1 with variation of soil thickness

The results of the S1 simulations are summarized in the first rows of Figs. 4, 5, and 6. By observing the basin-averaged water budget (Fig. 4a), it is evident that the variation in soil depth affects the change in the basin moisture over the simulation period, but not the basin discharge Q_t. Decreasing the soil depth decreases the basin's storage capacity and therefore the evaporation ET: this change is balanced energetically by an equal and opposite change in sensible heat H (Fig. 4b), while the ground heat flux, G, remains mostly unaltered. The simulations over the entire year with variations in soil thickness (Fig. 5a) show the same trends as the short-term simulations, but with no changes in ET and more changes in Q_t. In this case, the total annual precipitation input is larger than annual ET, as expected, and surface runoff is proportionally larger than subsurface flow, but this does not seems to affect the dependencies on soil thickness.

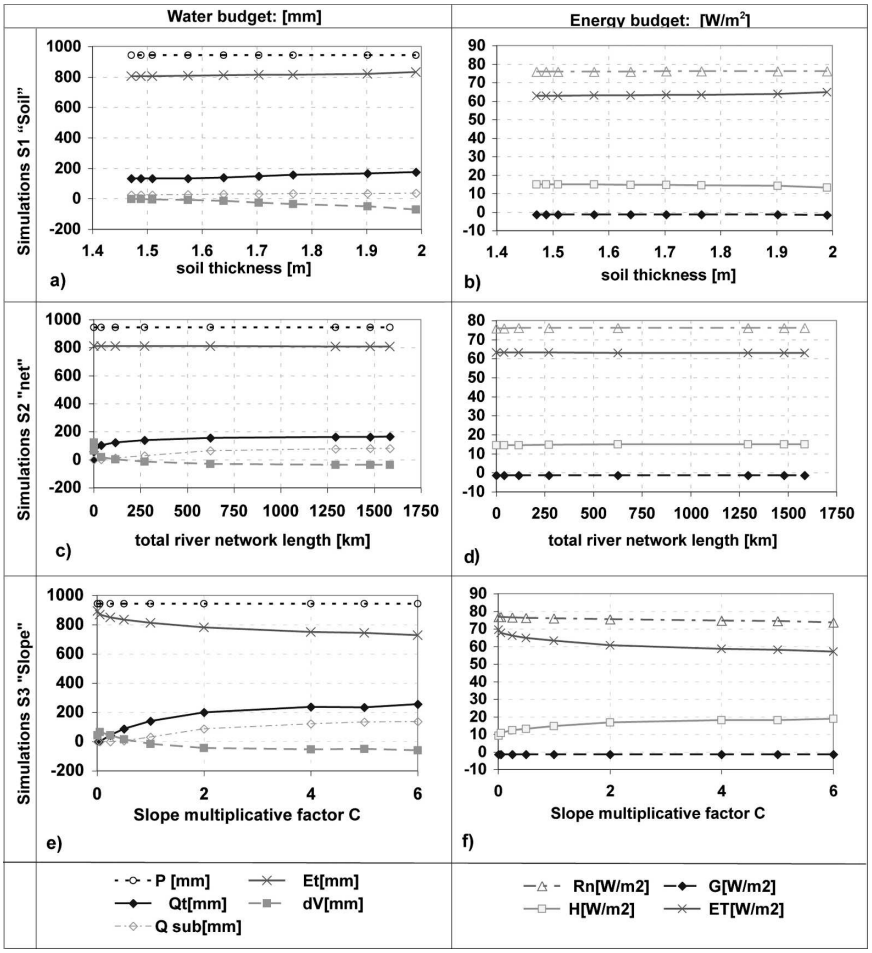

FIG. 5. Simulated (first column) total water budget and (second column) energy budget of the Little Washita watershed during 1997. (first row) Results of S1 simulations having soil thickness variation. (second row) Results of S2 simulations having river network variation. (third row) Results of S3 simulations having slopes modified by the factor c and consequent river network extension and soil thickness variation. Water budget and energy budget components are the same as in Fig. 4.

In Fig. 6 the ratio between Q_{sur}, water that reached the streams as overland flow and Q_{sub}, water that reached the streams as shallow subsurface flow, is shown. It is evident that most of the runoff is obtained as surface runoff, rather than subsurface (i.e., $Q_{\text{sur}}/Q_{\text{sub}} > 1$, with Q_{sur}/Q_{sub} taking a value of about 1.5 for runoff over the 27 June to 22 July simulation period and about 45 for the flood period), as a result of the flood on 11 July 1997. This ratio, furthermore, has a weak linear decrease (from 1.6 to 1.4, approximately, for the 27 June to 22 July period and from about 55 to 40 for the flood period) as the soil thickness increases, indicating a slight shift toward more subsurface runoff, as would be expected. Over the entire year this ratio shows almost no dependence on the geomorphic changes caused by the parameters varied in these experiments, has a constant ratio of 4, and is not reported in full. The time scale of Q_{sur} is, in fact, much shorter than one month, and therefore the yearly results are similar to the monthly ones.

b. *Results of S2 simulations with variation of river network extension*

The effects on water and energy budgets obtained by varying the river network extension are summarized in the second rows of Figs. 4, 5, and 6. As the mean celerity is far higher in the channels than in the hillslopes, it follows that, if the channel network extension is increased, the basin's drainage is more rapid (term dV in Fig. 4c), causing an increase of total discharge (term Q_t in Fig. 4c); moreover, once in channels, it is assumed in GEOtop that water cannot reinfiltrate.

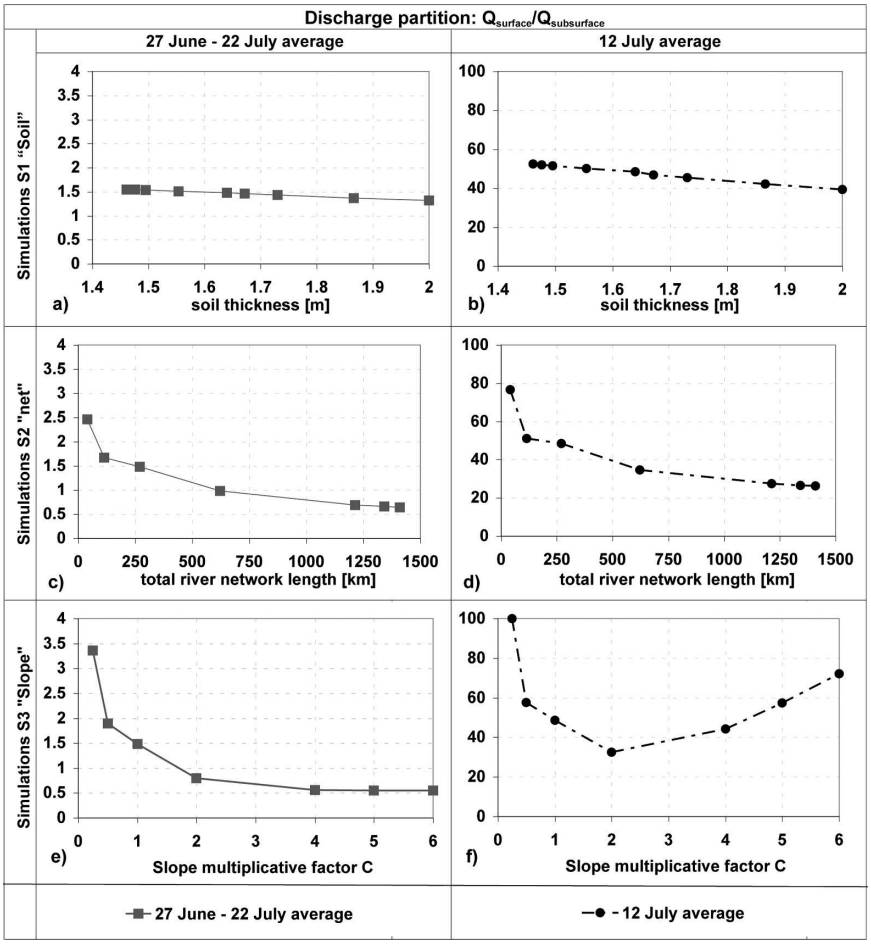

FIG. 6. Simulated runoff partition of the Little Washita watershed during the period 27 June–22 July 1997. The total discharge Q_t is partitioned into surface Q_{sur} and subsurface flow Q_{sub}, where $Q_t = Q_{sur} + Q_{sub}$. (first column) The ratio between surface and subsurface flow for the summer period simulated and (second column) the ratio for the day following the rainstorm of 11 July (12 July flood). (first row) Results of S1 simulations having soil thickness variation. (second row) Results of S2 simulations having river network variation. (third row) Results of S3 simulations having slopes modified by the factor c and consequent river network extension and soil thickness variation.

When the river network becomes vanishingly small, progressively larger amounts of overland flow, generated during the rainfall event, do not arrive at the outlet but reinfiltrate in the hillslopes. Thus Q_{sur} becomes negligible, as does Q_{sub}, because it is, by definition, dependent on the length of the channel network. Infiltrated water appears as water stored in soil (increasing dV) and would eventually flow through the outlet as base flow or evaporate, but this process would occur at a time scale longer than the simulations performed. For very little slope, water just evaporates or percolates into the groundwater system.

Regarding the water budget of the whole year, changing the network has significant effects on budget partition only when the river network is very short and little or no effects when the network is large. Moreover, the effect on ET during the whole year becomes, overall, almost negligible. Accordingly, the annual energy budget is almost unaffected by the river network increase. In the annual balance, ET remains much larger than sensible heat flux, whereas during the summer simulations they were approximately equal.

As shown in the second row of Fig. 6, for the summer period, the subsurface flow contribution to Q_t tends to increase more quickly with increasing channel network extension than does the surface runoff, resulting in a decreasing Q_{sur}/Q_{sub}. This effect has been described analytically in the case of flood events as a function of the drainage density in Rigon et al. (1996) and in D'Odorico and Rigon (2003). All individual events in

the annual simulations show the same qualitative result, and the relation of the total annual ratio versus the river network extension has the same shape as the plot in Fig. 6c but the ratio for the shorter river network is 10 instead of 2.5.

The increase in the discharge and decrease in basin water storage causes a corresponding but more slight decrease of the evaporation (term E_t in Fig. 4c), which is balanced by an equal and opposite change in the sensible heat flux, while the net radiation and ground heat flux remain substantially unchanged (Fig. 4d).

c. *Results of S3 simulations with variations of slope, river network extension, and soil thickness*

In this series of simulations, the slopes are varied, and so the soil thickness, according to Eq. (1), and the channel network extension, according to Eq. (2), varies along with the topography so that, along with steeper slopes, the soils get thinner (as in the S1 simulations) and the network extension becomes greater (as in the S2 simulations). All of these three changes contribute to a greater increase in the discharge (Fig. 4e), as compared to the case of the variation of soil depth or the channel network extension alone. The volume of evaporation decreases with steeper slopes; like the change in discharge, this change is larger than the one resulting from the effect of decreases in the soil depth or increases in the channel network extension alone.

For small slopes ($c \simeq 0$), the soils are deeper and the network vanishes as in the S2 simulations, so also $Q_t \simeq 0$. As the slopes are increased to small but nonzero values, there is a faster decrease in E_T than an increase in Q_t (because water tends to pond) so that dV increases to a maximum at $c = 0.25$ (Figs. 4e and 5e).

The variation in surface energy fluxes as a function of slope is shown in Fig. 4f. A peculiar effect of the topographic variation, as compared to the previous simulation series, is the slight diminution of the incident net radiation R_n. This diminution is due to the effects of shading, which begin to become noticeable in case of large local relief and which furthermore contributes to the diminution of the latent heat flux.

Slope variation also has remarkable effects on the annual water budget (Fig. 5e). Evapotranspiration decreases by around 15% and soil water storage also decreases; runoff and subsurface flow increase accordingly to match the budget. However, ET remains globally much larger than the other terms of the budget. In the energy budget (Fig. 5f), the decrease in ET and a very small decrease in the net radiation are mostly balanced by the increase in sensible heat transfer. In contrast to the short-term energy budget of the summertime period, ET remains much larger than H.

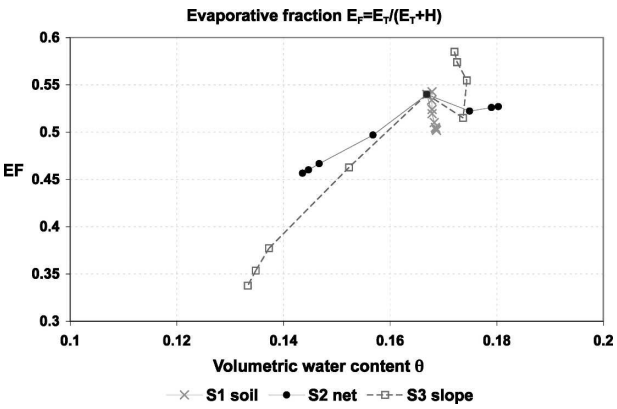

FIG. 7. Relation between basin-averaged evaporative fraction $E_F = E_T/(E_T + H)$ and the volumetric water content θ (averaged over the entire soil depth and over the whole simulation) in the Little Washita watershed for the three series of simulations S1 "soil," S2 "network," and S3 "slope" during the period 27 June–22 July 1997.

The variation of discharge partition between surface and subsurface flows as a function of slope is shown in the third row of Fig. 6. During the summer simulation period (27 June–22 July), Q_{sur}/Q_{sub} decreases. Over the entire year 1997 the ratio decreases as well, as seen in the results of the previous S2 simulations series. During the flood event (12 July), Q_{sur}/Q_{sub} has a minimum for $c = 2$; however, with increasing c, peak discharge becomes strongly dominated by surface runoff, Q_{sur}.

d. *Discussion*

An interesting additional perspective on the results of these simulations is provided by the analysis of the relation between the basin-average evaporative fraction $E_F = E_T/(E_T + H)$ and the volumetric water content θ (averaged over the whole soil depth), shown in Fig. 7 for the summer period and in Fig. 8 for the entire year. During the summer period, if the topography varies, and with it the soil thickness and the channel net extension (i.e., the S3 simulations), for very small variations in average basin saturation (less than 10%), there exists a significant difference in evaporation fluxes (up to 40%), as shown in Fig. 7. However, the evaporative fraction is not very sensitive to the variations of the soil depth alone (the S1 simulations) and is only moderately sensitive to the extension of the channel network alone (the S2 simulations). The same E_F, analyzed over the entire year of 1997, shows larger values but a more limited variation with increasing slope (between 0.74 and 0.9). Mean annual water volumetric water content is also larger than mean summer water content, as expected; thus the annual E_F versus θ curves are shifted toward the upper-right part of the plane. Increasing soil

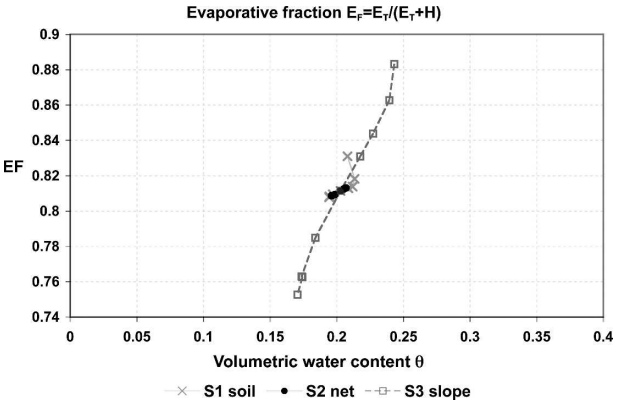

FIG. 8. Relation between basin evaporative fraction $E_F = E_T/(E_T + H)$ and the volumetric water content θ in the Little Washita watershed for the three series of simulations S1 "soil," S2 "network," and S3 "slope" during the entire year 1997.

depth and river network extension alone does not noticeably affect E_F. These elements of heterogeneity are generally overlooked in global models. The Little Washita watershed, with an area of about 600 km^2, in fact has a size much smaller than a single element of a typical global atmospheric circulation model (GCM) in which the evaporative fluxes are summarized in a single value. In a large-scale model, the decrease of residence time of surface and subsurface storm waters due to a steeper topography can be absorbed with a proper increase of the apparent surface and subsurface water flow celerities (which can be obtained with a suitable calibration) and the decrease of storage with an increase of runoff production [which, in turn, in models derived from TOPMODEL (Beven and Kirkby 1979), such as TOPLATS (Famiglietti and Wood 1994), can be simulated by a faster decrease of conductivity with depth]. The case of evapotranspiration reveals a nonlinear trend with stored moisture for the shortest time scale. However, the nonlinearity is less important at the annual time scale. Because, to a first approximation, the sum of latent and sensible heat remains constant (and the change in energy storage both at the weekly and seasonal time scale seems to be negligible), the effect of heterogeneity is a variation of the Bowen ratio (the ratio of sensible to latent heat fluxes).

A different representation of the water budget, as a monthly time series (Fig. 9), allows also for some further considerations. With little basin relief ($c = 0.01$), there is no river network and the discharge is negligible. Evaporation is consequently increased, clearly depending also on available solar radiation. As slopes steepen, discharges increase in wet months much more than in dry months. This change is compensated by a decrease of ET and water storage. Moreover, the increase of ET in summer months is larger for the flatter topographies. Finally, steeper topographies show smaller storage capacities during the wetter periods but also greater storage capacity in summer. This is the consequence of the concentration of residual soil water in concave lowlands

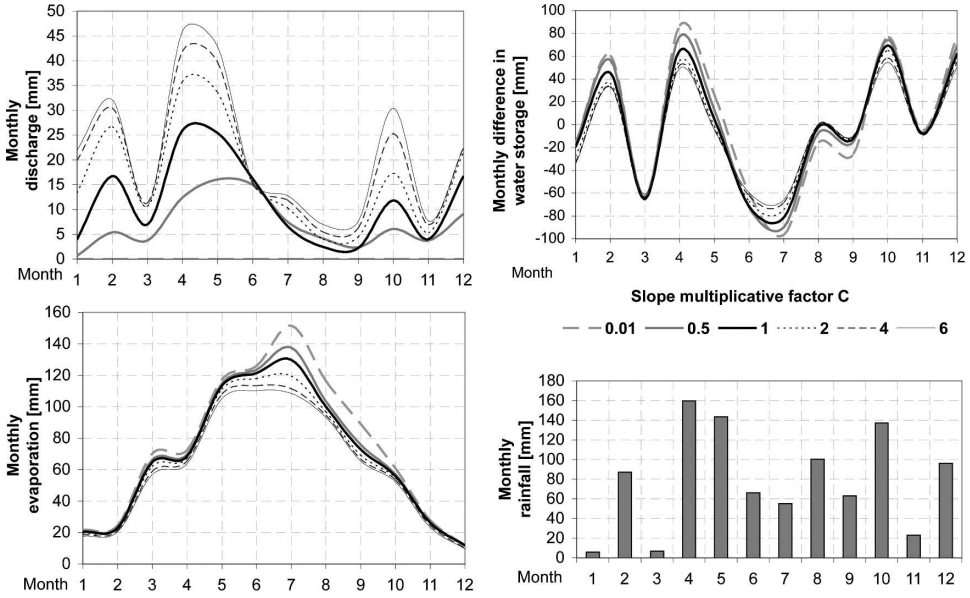

FIG. 9. Monthly water balance for the Little Washita basin in year 1997 for real ($c = 1$) and modified topographies. For geomorphic properties of the different simulations, see Table 3. Basin discharge, monthly difference in water storage, evaporation, and rainfall are reported.

for steeper topography and of a relative more spatially uniform soil water distribution in flatter topographies. The sensitivity of water and energy budgets to topography is clearly larger in the wettest and driest periods and considerably larger at the monthly as compared to the annual time scale.

4. Annual water and energy budgets in the Serraia lake basin

To understand the effect of geomorphic changes over the annual cycle in a small mountain basin, where topography has major effects and different climatic conditions are present, the same methodology has been applied to the Serraia basin (Trentino, Italy), a mountain basin where the data was collected for the whole year 2000 (Forlin 2001). This basin is located in the Italian Alps and has an area of 9 km^2 and an elevation range between 900 and 1900 m, the steep slopes making the effects of aspect, shadowing, and sky view on net radiation quite significant (Figs. 1 and 3). The basin's hydrological cycle has been estimated on the basis of measurements that include meteorological data (air temperature at 1.5 m, wind speed at 5 m, shortwave radiation, and air humidity) and streamflow. GEOtop was calibrated against discharge in the Foss Grand subcatchment (Fig. 1). Meteorological data are measured at a station in the bottom of the valley (Fig. 1). Temperature was assumed to vary linearly with elevation according to a lapse rate of 0.6°C per 100 m. Wind velocity has been assumed spatially constant.

Using the S3 simulations approach ("variable slope"), it is possible to simulate the effects of slope variation, along with a consequent variation of river network extension and soil depth, for the Serraia catchment, as shown in Fig. 1 and Table 4. The total annual water budget of the Serraia catchment shows the same behavior as the Little Washita watershed: an increase in slope causes an increase in discharge and a decrease in evapotranspiration, as reported in Fig. 10. However, unlike the Little Washita where evapotranspiration greatly exceeds discharge, over the annual cycle at Serraia, discharge and evapotranspiration are of comparable magnitude and present linear trends with variation of parameter *c*.

The monthly budgets for the Serraia are shown in Fig. 11. It appears that the Serraia basin during the year 2000 is affected by a greater seasonality than Little Washita during the year 1997. The first part of the year was quite dry, followed by a very wet fall. All simulations show a similar low flow during dry months and a similar high flow in November (month 11 in Fig. 11), the month with maximum precipitation. However, the maximum difference in monthly discharges among simulations occurs in the previous month of October when the maximum difference of soil water storage among the simulations occurs (arrow in Fig. 11, upper-left panel). Basins with gentler slopes and deeper soil ($c = 0.25$) preserve soil moisture a month longer than those with steeper slopes and therefore shallower soil ($c = 1.25$). A possible explanation is that October precipitation was enough to mostly fill the storage capacity of the basins with steeper slopes, but not enough to saturate the flatter basins (having deeper soil and a less developed river network), which continue to store water in soils also during November. This variation in water balance due to topographic and geomorphic factors is at least as important as the moisture variations induced by climatic variability.

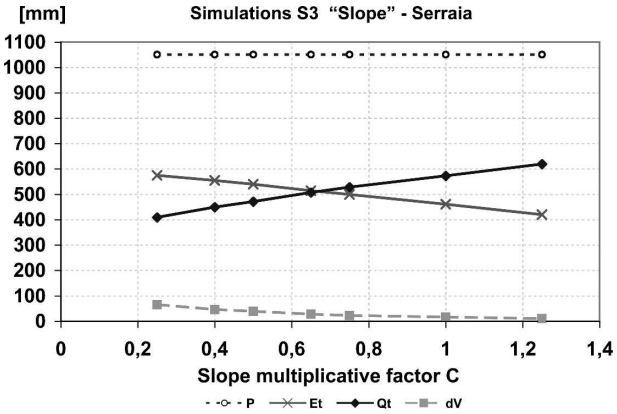

FIG. 10. Simulated total water budget of the Little Serraia catchment during the year 2000 for simulations S3 ("slope") with slope, river network, and soil thickness variation. Water budget components are precipitation *P,* evaporation E_T, change in soil water content variation *dV,* and total discharge Q_t. For geomorphic properties of the different simulations, see Table 4.

5. Conclusions

The presence of topographic and topographic-induced geomorphic variations of quantities such as the extension of the channel network or the soil storage (both of which may be caused by diverse topographies in real landscapes) are shown to exert a direct control on the water storage in the hillsides and consequently on the quantity and rate of production of surface and subsurface runoff and on the evapotranspiration. Through the GEOtop simulations described, it has been observed that both a more extended channel network and steeper slopes determine an increase in the discharge and an opposite diminution of the evapotranspiration. The same effects are observed in the Little Washita watershed during a simulation of a summer month and on the longer yearly scale both at the

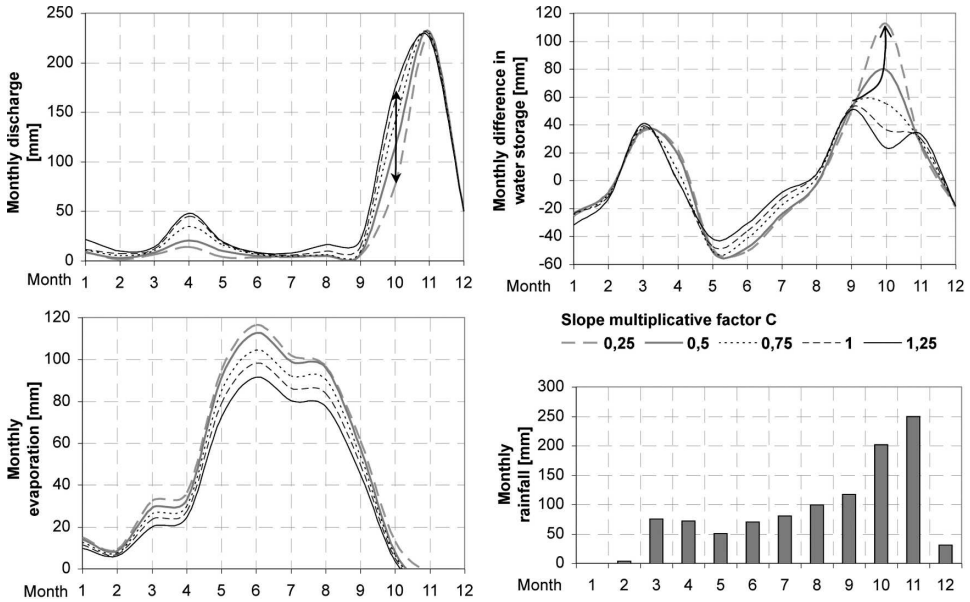

FIG. 11. Monthly water balance for the Serraia basin in year 2000 for real (c = 1) and modified topographies. For geomorphic properties of the different simulations, see Table 4. Basin discharge, monthly difference in water storage, evaporation, and rainfall are reported. Notice the wet fall period. Arrows indicate the maximum difference among simulations with real and modified topography.

Little Washita and at the Serraia Lake catchment. The summer simulations show effects on the water and energy budget partition that tend to smooth at the annual time scale. In all of the cases, the decrease of latent heat fluxes is balanced by an increase in the sensible heat flow and negligible variation of the other fluxes. However, in the Little Washita watershed a slight decrease of the incident net radiation due to the increase in shading with slope is observed. Furthermore, it has been observed that in the Little Washita watershed the partition between runoff and subsurface fluxes changes when the slope increases in favor of the latter, except during flood periods when increased slope produces more surface runoff, and the surface runoff is more concentrated in time.

At the annual time scale, just the difference in topography was observed to significantly affect the water budget. Nevertheless, the variations in the total annual budgets are less relevant than those induced in the monthly budgets; the persistent variations in the latter, induced by persistent topographic characteristics as opposed to climatic fluctuations, have important consequences on flood frequency and ecosystems fitness, too large to be neglected.

In the end, it has been observed that the linear relations that link the local evapotranspiration to the local soil moisture do not always remain valid for the whole basin, if total evapotranspiration and averaged soil moisture are used. In fact, for very small variations in averaged basin saturation, significant differences in evaporation fluxes were observed. Therefore it is suggested that new subgrid parameterizations of large-scale LSMs, dependent on topography, are required.

Acknowledgments. We thank the Civil and Environmental Engineering Department of the University of Illinois at Urbana–Champaign and the Illinois Water Sciences Center of the USGS for their hospitality during the visit of the first author during the course of this research. This research was partially supported by the Italian Ministry of University and Research (MIUR Prin 2003) and by the European Union within the 5th Framework TIDE project, Contract EVK3-CT-00064, and within the 6th Framework AQUATERRA project. The Agricultural Research Service, Grazinglands Research Laboratory (ARS-GRL), El Reno, Oklahoma, provided the Little Washita precipitation data, and the ARS-GRL, in cooperation with the USGS and the Oklahoma Water Resources Board, provided the Little Washita discharge data.

APPENDIX

A Derivation of the Soil Depth Based on a Linear Diffusion Theory

The model assumes that the mass balance equation relative to a soil column can be written as

$$\rho_s \frac{\partial h}{\partial t} + \rho_r \frac{\partial z}{\partial t} = -\nabla \cdot \rho_s q_s, \tag{A1}$$

where h is the soil depth, z is the bedrock surface elevation, t is time, ρ_r (M L^{-3}) and ρ_s (M L^{-3}) are the rock and soil bulk densities respectively, ∇ is the gradient operator (L^{-1}), and q_s (L^2 T^{-1}) is the rate of soil erosion for unit hillslope width. A reasonable assumption for soil creation is given by Heimsath et al. (1997):

$$\frac{\partial z}{\partial t} = -P_0 e^{-mh}, \tag{A2}$$

where P_0 (L T^{-1}) is the soil production for null soil depth and m the decay rate with soil depth of soil production (L^{-1}). According to Heimsath et al. (1997), the erosion law is given by

$$q_s = -k\nabla z, \tag{A3}$$

where k (L^2 T^{-1}) is a soil diffusivity factor. A rationale for using this law, which assumes additive random factors to produce the transport, and its limits are discussed in Rodriguez-Iturbe and Rinaldo (1997) and Scheidegger (1991). If there is a stationary balance between soil production and erosion, the soil depth remains constant and $\partial h/\partial t = 0$; then, after substitution of (A2) and (A3) in (Al) the equation reduces to

$$-\rho_r P_0 e^{-mh} = k\rho_s \nabla^2 z, \tag{A4}$$

which can be easily inverted as in (1) and implies that a stationary soil production can be obtained only in hillslope where $\nabla^2 z \leq 0$ (this would be true for any type of soil production being defined positive). Equation (A4) refers to a point. When integrating a whole area and denoting the spatial average with angle brackets, we have

$$\langle e^{-m(\langle h\rangle + h')}\rangle = -\left\langle k\frac{\rho_s}{\rho_r P_0}\nabla^2 z\right\rangle, \tag{A5}$$

where $h \equiv \langle h\rangle + h'$ decomposes the soil depth into its spatial average plus a fluctuation. The left member of (A5) is a mean that can be expressed as

$$\langle e^{-m(\langle h\rangle + h')}\rangle = e^{-m\langle h\rangle}\langle 1 - mh' + (1/2)m^2 h'^2 - (1/6)m^3 h'^3 \cdot \cdot \cdot\rangle. \tag{A6}$$

Assuming that the distribution of h' around the mean $\langle h\rangle$ is symmetric, all odd terms in (A6) are zero and the term in angle brackets can be written as an exponential of fluctuations variances, σ_h and

$$e^{-m(\langle h\rangle - 0.5m\sigma_h^2)} = -\left\langle k\frac{\rho_s}{\rho_r P_0}\nabla^2 z\right\rangle. \tag{A7}$$

Finally, from (A7) the soil depth Eq. (1) can be easily derived by setting $\sigma_h = 0$ and assuming homogeneous soil properties inside grid cells. Thus, the heterogeneous soil depth inside a cell gives a positive contribution to mean soil depth. The presence of an asymmetric distribution, since the odd terms in (A6) are all negative, decreases the soil depth. However, since the higher the moment, the lesser its contribution to the summation in (A6), the total effect of heterogeneity is to increase the mean soil depth.

REFERENCES

Albertson, J., W. P. Kustas, and T. M. Scanlon, 2001: Large-eddy simulation over heterogeneous terrain with remotely sensed land surface conditions. *Water Resour. Res.,* **37,** 1939–1953.

Avissar, R., and R. A. Pielke, 1989: A parameterization of heterogeneous land surfaces for atmospheric numerical models and its impact on regional meteorology. *Mon. Wea. Rev.,* **117,** 2113–2136.

Beven, K. J., and M. J. Kirkby, 1979: A physically-based variable contributing area model of basin hydrology. *Hydrol. Sci. Bull.,* **24,** 43–49.

Carson, M. A., and M. Kirkby, 1972: *Hillslope Form and Process.* Cambridge University Press, 475 pp.

Dietrich, W. E., C. J. Wilson, D. R. Montgomery, and J. McKean, 1993: Analysis of erosion thresholds, channel networks, and landscape morphology using a digital terrain model. *J. Geol.,* **101,** 161–180.

D'Odorico, P., and R. Rigon, 2003: Hillslope and channel contributions to the hydrologic response. *Water Resour. Res.,* **39,** 1113, doi:10.1029/2002WR001708.

Entekhabi, D., and P. Eagleson, 1989: Land surface hydrology parameterization for atmospheric general circulation models including subgrid scale spatial variability. *J. Climate,* **2,** 816–831.

——, I. Rodriguez-Iturbe, and R. L. Bras, 1992: Variability in large-scale water balance with land surface–atmosphere interactions. *J. Climate,* **5,** 798–813.

Famiglietti, J. S., and E. F. Wood, 1994: Multiscale modeling of spatially variable water and energy balance processes. *Water Resour. Res.,* **30,** 3061–3078.

Forlin, L., 2001: Varie applicazioni di un modello di bilancio idrologico. Tesi di diploma, Corso di diploma in Ingegneria per l'Ambiente e le Risorse, University of Trento, 128 pp.

Heimsath, M. A., W. E. Dietrich, K. Nishiizumi, and R. Finkel, 1997: The soil production function and landscape equilibrium. *Nature,* **388,** 358–361.

Jackson, T. J., D. M. LeVine, A. Hsu, A. Oldak, P. Starks, C. Swift, J. Isham, and M. Haken, 1999: Soil moisture mapping at regional scales using microwave radiometry: The Southern Great Plains Hydrology Experiment. *IEEE Trans. Geosci. Remote Sens.,* **37,** 2136–2151.

Lakshmi, V., J. Albertson, and J. Schaake, Eds., 2001: *Land Surface Hydrology, Meteorology, and Climate: Observations and Modeling.* Amer. Geophys. Union, 246 pp.

Liang, X., D. Lettenmaier, E. Wood, and S. Burges, 1994: A simple hydrologically based model of land surface water and energy fluxes for general circulation models. *J. Geophys. Res.,* **99** (D7), 14 415–14 428.

Mohanty, B. P., J. Famiglietti, and T. Skaggs, 2000: Evolution of

soil moisture spatial structure in a mixed-vegetation pixel during the SGP97 Hydrology Experiment. *Water Resour. Res.,* **36,** 3675–3686.

Mohr, K. I., J. S. Famiglietti, A. Boone, and P. Starks, 2000: Modeling soil moisture and surface flux variability with an untuned land surface scheme: A case study from the Southern Great Plains 1997 Hydrology Experiment. *J. Hydrometeor.,* **1,** 154–169.

Prosser, I. P., and B. Abernethy, 1996: Predicting the topographic limit to a gully network using a digital terrain model and process thresholds. *Water Resour. Res.,* **32,** 2289–2298.

Rigon, R., P. D'Odorico, and L. Parra, 1996: Metodi geomorfologici di inferenza della risposta idrologica. *Proc. Atti del XXV Convegno Nazionale di Idraulica e Costruzioni Idrauliche,* Torino, Italy.

——, G. Bertoldi, and T. M. Over, 2006: GEOtop: A distributed hydrological model with coupled water and energy budgets. *J. Hydrometeor.*, **7,** 371–388.

Rodriguez-Iturbe, I., and A. Rinaldo, 1997: *Fractal River Basins: Chance and Self-Organization.* Cambridge University Press, 547 pp.

——, P. D'Odorico, A. Porporato, and L. Ridolfi, 1999: On the spatial and temporal links between vegetation, climate, and soil moisture. *Water Resour. Res.,* **35,** 3709–3722.

Scheidegger, A. E., 1991: *Theoretical Geomorphology.* 3d ed. Springer, 434 pp.

Stocker, R., 1998: Sull'utilizzo delle mappe digitali del terreno nello studio della risposta idrologica. Master's thesis, Università degli Studi di Padova, 95 pp.

Warrach, K., M. Stieglitz, H. Mengelkamp, and E. Raschke, 2002: Advantages of a topographically controlled runoff simulation in a SVAT model. *J. Hydrometeor.,* **3,** 131–148.

Wigmosta, M. S., L. Vail, and D. Lettenmaier, 1994: A distributed hydrology–vegetation model for complex terrain. *Water Resour. Res.,* **30,** 1665–1679.

Willgoose, G., R. L. Bras, and I. Rodriguez-Iturbe, 1991: A physically based coupled channel network growth and hillslope evolution model, 1, Theory. *Water Resour. Res.,* **27,** 1671–1684.

Zanotti, F., S. Endrizzi, G. Bertoldi, and R. Rigon, 2004: The GEOTOP snow module. *Hydrol. Processes,* **18,** 3667–3679.